Enhanced Intersystem Crossing in Donor/Acceptor Systems Based on Zinc/Iron or Free-Base/Iron Porphyrins

Kristine Kilså,[a] Johan Kajanus,[b] Sven Larsson,[a] Alisdair N. Macpherson,[c] Jerker Mårtensson,[b] and Bo Albinsson*[a]

Abstract: The deactivation pathways of the singlet excited state of a series of zinc or free-base donor porphyrins covalently linked by a bridge to a paramagnetic iron(III) chloride porphyrin acceptor have been studied. These donor-bridge-acceptor systems all share a similar geometry (25 Å donor–acceptor center-to-center distance), but the bridges vary in electronic structure. In previously reported investigations of zinc/iron porphyrin systems, the fluorescence quenching of the donor has predominantly been assigned to electron transfer. However, for the porphyrin systems studied in this paper, we show that the dominant deactivation channels are enhanced intersystem crossing and singlet energy transfer. In both series, the intersystem crossing rate ($S_1 \rightarrow T_1$) of the donor moiety is almost doubled in the presence of a paramagnetic high-spin metal-porphyrin acceptor. The significant spectral overlap of the donor fluorescence and acceptor absorption in both series allows for efficient singlet energy transfer (Förster mechanism). Furthermore, the bridging chromophores mediate energy transfer and the enhancement is inversely dependent upon the energy gap between the donor and bridge excited states. Although Marcus theory predicts thermodynamically favorable electron transfer to occur in the systems investigated, the quenching rate constants were found to be independent of solvent polarity, and no charge-separated state could be detected, indicating very small electronic coupling for electron transfer.

Keywords: donor–acceptor systems · electron transfer · intersystem crossing · mediated energy transfer · porphyrinoids

Introduction

To efficiently capture, store, and beneficially use solar energy is a goal of numerous projects, which involve, for example, the construction of artificial light-harvesting complexes,[1–4] photosynthetic reaction-center mimics,[5–8] and opto-electronic devices.[9, 10] Much of this work has been inspired by Nature's transportation of excitation energy[11, 12] and conversion into long-distance charge-separated states.[13] In order to understand the primary photophysical processes involved, it is important to gain knowledge, and thereby control, of the parameters that influence energy- and electron-transfer rates. To investigate the mechanisms of photoinduced excitation energy and electron transfer,[14, 15] various supramolecular complexes have been constructed, with particular emphasis on the effects of donor–acceptor distance[16–18] and orientation,[19–21] free energy of reaction,[22, 23] temperature,[24–27] and electronic coupling.[28, 29] The success of such investigations depends on the ability to separate and isolate factors that influence the transfer processes. In the work presented here, the increased fluorescence quenching of the singlet excited donor state in donor-bridge-acceptor systems, relative to the reference donor-bridge compounds, are investigated and related to possible deactivation pathways.

The systems we have studied are geometrically well-defined donor-bridge-acceptor (D-B-A) systems (Figure 1). Both donor and acceptor are porphyrins and they are covalently connected by four different bridging chromophores. In addition to acting as an intervening medium, the bridging chromophores serve as rigid spacers between the donor and acceptor and place geometrical constraints on the system. The donor is either 5,15-diphenyl-2,8,12,18-tetraethyl-3,7,13,17-

[a] Dr. B. Albinsson, Dr. K. Kilså, Prof. S. Larsson
Department of Physical Chemistry
Chalmers University of Technology
412 96 Göteborg (Sweden)
Fax: (+46) 31-772-3858
E-mail: balb@phc.chalmers.se

[b] Dr. J. Kajanus, Dr. J. Mårtensson
Department of Organic Chemistry
Chalmers University of Technology
412 96 Göteborg (Sweden)

[c] Dr. A. N. Macpherson
Department of Biophysical Chemistry
Umeå University, 901 87 Umeå (Sweden)

Supporting information for this article is available on the WWW under http://www.wiley-vch.de/home/chemistry/ or from the author. ^{1}H NMR spectra of FeP, FeP-OB, FeP-BB, FeP-NB, FeP-AB, ZnP-OB-FeP, ZnP-BB-FeP, ZnP-NB-FeP, and ZnP-AB-FeP.

  0947-6539/01/0710-2122 $ 17.50+.50/0

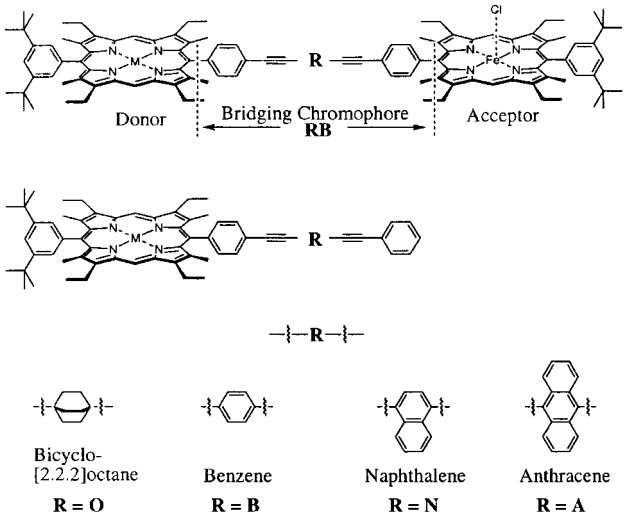

Figure 1. Structure of the donor-bridge-acceptor (D-B-A) systems and the reference compounds (donor-bridge or acceptor-bridge) studied. The D-B-A systems (M = Zn or 2H) are denoted ZnP-RB-FeP or H_2P-RB-FeP, respectively. The reference compounds (M = Zn, 2H, or Fe) are denoted ZnP-RB, H_2P-RB, or FeP-RB, respectively. RB is the bridging chromophore in which R is the central unit, which is either bicyclo[2.2.2]octane (O), benzene (B), naphthalene (N), or anthracene (A).

tetramethylporphyrin (H_2P), or the corresponding zinc porphyrin (ZnP), and the acceptor is the similar high-spin iron(III) chloride porphyrin (FeP). Three of the four bridging chromophores are fully conjugated systems: bis(phenylethynyl)-1,4-phenylene (BB), bis(phenylethynyl)-1,4-naphthylene (NB) or bis(phenylethynyl)-9,10-anthrylene (AB), while the fourth bridging chromophore, bis(phenylethynyl)-1,4-bicyclo[2.2.2]octylene (OB), is non-conjugated.

Scheme 1 shows the possible deactivation pathways of the singlet excited donor state in the D-B-A systems. In addition to energy and electron transfer from the lowest singlet excited state of the donor moieties to the acceptor, intramolecular

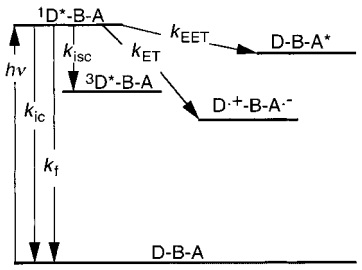

Scheme 1.

deactivation processes such as fluorescence, internal conversion, and intersystem crossing also contribute to the deactivation of the donor. Since one part of the D-B-A system is a paramagnetic (high-spin) metal porphyrin, it has not only the possibility of acting as an energy or electron acceptor, but potentially it may also be able to influence intersystem crossing in the donor.[30, 31] Several other donor–acceptor systems with zinc and iron(III) porphyrins have been studied recently and in these systems, it was concluded that electron transfer is the major deactivation pathway for the zinc-porphyrin singlet excited state.[16, 18, 21, 32–35] Long-range electron transfer from a triplet excited zinc porphyrin to an iron porphyrin has also been shown to occur in systems with 25 Å donor–acceptor distance, in which it was believed that electron transfer from the singlet excited donor state could not occur.[36] Systems containing free-base and iron(III) porphyrins are not commonly investigated.[37] We have, however, made a comparative study of both systems: zinc/iron and free-base/iron porphyrin. Attempts have been made to study electron transfer and other possible photophysical pathways of singlet-excited donor deactivation.

Results

Synthesis: The syntheses of the ZnP-RB-H_2P systems and the corresponding reference compounds (ZnP-RB, H_2P-RB, ZnP and H_2P), used in studies of excitation energy transfer, have been described previously.[28, 38] These systems were prepared by using a palladium-catalyzed cross-coupling reaction between terminal alkynes and aromatic iodides,with [$Pd_2(dba)_3$] as the catalyst precursor and $AsPh_3$ as ligand.[39]

The ZnP-RB-FeP dimers were prepared in one step from the ZnP-RB-H_2P analogues by iron insertion into the free base part of the dimer. We also prepared the separate acceptor (FeP) and the acceptor-bridge compounds (FeP-RB) from H_2P and H_2P-RB, respectively. These latter compounds were prepared to determine the effect of the connected bridge on the optical properties of the acceptor. This effect was shown to be small (vide infra). The FeP and FeP-RB compounds were also useful in the interpretation of the ^{1}H NMR spectra (Figure 2).

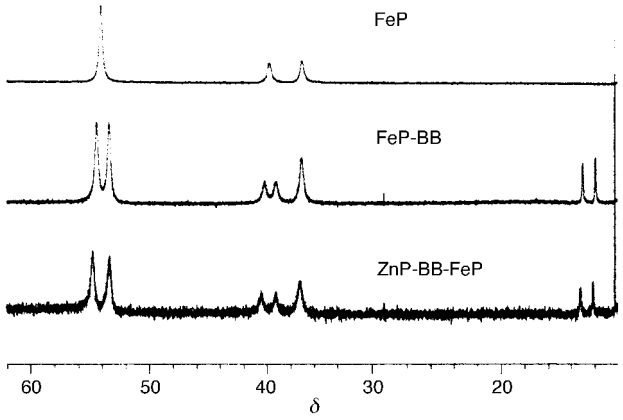

Figure 2. Downfield region of the ^{1}H NMR spectra of FeP, FeP-BB, and ZnP-BB-FeP in $CDCl_3$. Downfield shifts are given a positive sign. The peak of highest intensity at $\delta = 10$ is due to the *meso*-protons of ZnP in ZnP-BB-FeP.

The zinc-porphyrin moiety is rapidly de-metalated under acidic conditions and so iron insertion into the free-base part of the ZnP-RB-H_2P dimer needs to be performed under basic conditions. The method used by Young and Chang[40] (treatment of a free-base porphyrin with $FeBr_2$ in toluene/THF by using collidine as base) proved satisfactory for the preparation of FeP and FeP-RB. The axial bromide ligand was exchanged for chloride by treatment with 10% hydrochloric acid.

The same procedure was used for the preparation of the ZnP-RB-FeP dimers, with $FeCl_2$ as the metalating agent; this allowed direct preparation of the iron porphyrin moiety as the iron(III) chloride complex without acid treatment. The crude product was purified by chromatography on alumina to remove a strongly colored byproduct that is as yet unidentified, but is of porphyrin origin. The product was further purified by chromatography on silica to remove starting material. Occasionally, a small fraction of the ZnP-RB-FeP dimers was de-metalated to the H_2P-RB-FeP dimer during chromatography on silica; this was only detectable by fluorescence measurements. Therefore, zinc insertion was routinely performed as a final step in the preparation of the ZnP-RB-FeP dimers. It was evident in the ^{1}H NMR spectra that some ligand scrambling of the iron(III) porphyrin occurred during workup. The axial chloride ligand could, however, be re-established by washing a solution of the dimer in ethyl acetate with saturated aqueous ammonium chloride. Following recrystallization from dichloromethane/hexane, the ZnP-RB-FeP dimers were obtained in about 40% yield. The H_2P-RB-FeP dimers were prepared from the ZnP-RB-FeP dimers by treatment with 10% hydrochloric acid.

^{1}H NMR spectroscopy of iron porphyrins: The ZnP/FeP bisporphyrins prepared previously have generally not been characterized by ^{1}H NMR spectroscopy.[16, 18, 21, 32–35] However, we found it useful to utilize the proton signals of the ring-methyl and -ethyl groups of the porphyrins investigated here as diagnostic tools to establish that the iron porphyrin was the high-spin iron(III) chloride porphyrin. The ^{1}H NMR spectrum of FeP is indicative of a high-spin complex, showing a strong resemblance to the proton spectra of high-spin etioporphyrin chlorides[41] and diphenyletioporphyrin chlorides (Figure 2).[40] Based on a comparison with such porphyrins, we assign the peak at $\delta = 54$ (downfield shifts are given a positive sign) in the spectrum of FeP to the ring-methyl group and the peaks at $\delta = 40$ and 37 to the CH_2 group of the ring-ethyl groups. The spectra of the unsymmetrical FeP-RB porphyrins show the same general features, but the ring-methyl signal is split into two peaks at $\delta = 54$ and 53, and one of the CH_2 signals is also split. The same pattern is again observed for the ZnP-RB-FeP dimers. In the spectra of FeP-RB and ZnP-RB-FeP there are additional peaks with downfield shifts at $\delta = 12$ and 13. We assign these signals to the protons in a *meta* position, relative to the porphyrin, on the 1,4-substituted phenyl ring attached to the iron porphyrin. The signals from the protons in the *ortho* position are probably too severely broadened to be detectable.

The ^{1}H NMR spectra of the dimers recorded before treatment with ammonium chloride contain peaks of low intensity centered at $\delta = 30$ and 40. This indicates that the iron porpyrin moiety has to some extent been converted to the OH^-[40] or possibly an alkoxide complex. There is also the possibility of the formation of a μ-oxo-bridged complex with an oxygen linking two iron(III) porphyrins together forming a porphyrin tetramer. However, μ-oxo dimers of iron porphyrins are known to be too strongly coupled to give rise to such large downfield shifts as $\delta = 30$ to 40.[40, 41] In the ^{1}H NMR spectra of the final products there are no signals indicating the presence of any iron porphyrin species other than the iron(III) chloride porphyrin.

Structural considerations: Since the systems investigated here are similar in structure to the previously studied excitation-energy-transfer systems (ZnP-RB-H_2P),[28, 42] we believe that the following structural properties of the latter are applicable: i) The center-to-center distance from donor to acceptor is constant (25 Å) throughout the series. ii) The low rotation barriers (< 1 kcal mol^{-1}) of the bridging chromophores make all relative orientations of bridge and porphyrin planes energetically attainable at room temperature and the relative orientation of the donor and the acceptor independent of the bridging chromophore. iii) Simple π conjugation through the system is minimized by placing methyl groups on the porphyrin rings adjacent to the phenyl substituents, thereby placing steric constraints on the dihedral angle (ω) between the porphyrin and phenyl planes. From PM3 calculations on H_2P with fixed dihedral angles, ω can be estimated to be $90^\circ \pm 18^\circ$ at 300 K, narrowing down to $90^\circ \pm 11^\circ$ at 100 K (90% of the conformers according to the Boltzmann distribution). This helps to preserve the identities of the donor, bridge, and acceptor chromophores, which is confirmed by the fact that the D-B-A absorption spectra can be resolved into the spectral sum of the three chromophores, or equally well into the sum of D-B and A (Figure 3). The spectra of FeP-RB reference compounds are, for $\lambda > 500$ nm, identical to the spectrum of FeP (data not shown); however, the internal charge-transfer bands are sharper than those found for the FeP chromophore in the D-B-A systems. This is probably due

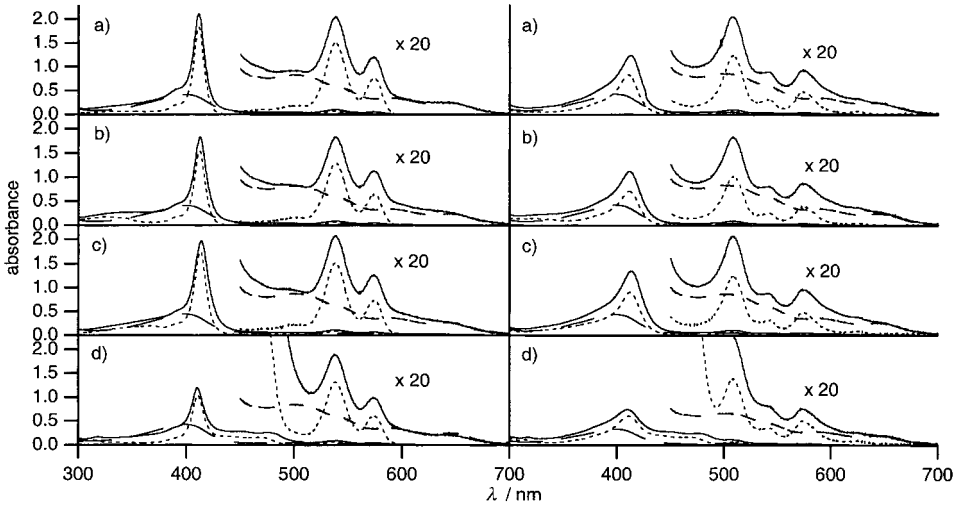

Figure 3. Absorption spectra of D-B-A systems (——), donor (- - - -) and acceptor (– – –) references in $CHCl_3$, 20 °C. From top to bottom, with D = ZnP (left) and D = H_2P (right): a) D-OB-FeP, D-OB, and FeP; b) D-BB-FeP, D-BB, and FeP; c) D-NB-FeP, D-NB, and FeP; d) D-AB-FeP, D-AB, and FeP.

0947-6539/01/0710-2124 $ 17.50+.50/0 *Chem. Eur. J.* **2001**, *7*, No. 10

to the presence of a near-degenerate porphyrin in the D-B-A systems. For systems containing the AB bridge, the resolution into spectral compounds is only valid in the Q-band region ($\lambda > 500$ nm), since the excited states of the porphyrin Soret band and AB are isoenergetic. Therefore, the samples were always excited at a wavelength longer than 500 nm at which the absorption of donor dominated. However, excitation of the acceptor will not influence the analysis, since the acceptor is nonfluorescent and has a very short excited-singlet-state lifetime (ca. 2.7 ps, data not shown).

Total deactivation rate of the donor singlet excited state: Figure 4 shows the steady-state fluorescence spectra in $CHCl_3$ of all the D-B-A systems compared to the fluorescence

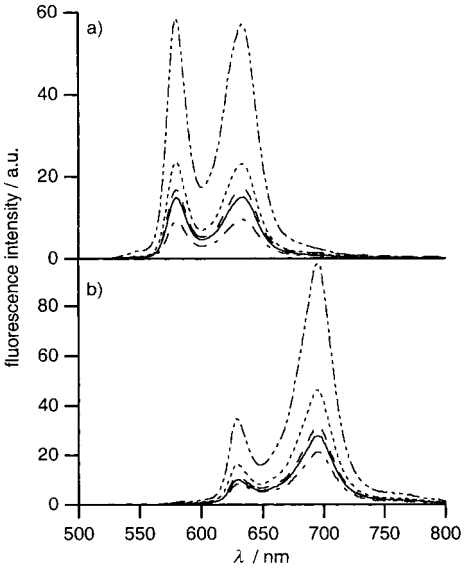

Figure 4. Fluorescence emission spectra of the D-B-A systems compared with the fluorescence spectrum of the donor (scaled to equal donor optical density) in $CHCl_3$, 20 °C. a) D = ZnP, b) D = H_2P: D(–••–), D-OB-FeP (••••), D-BB-FeP (– – –), D-NB-FeP (——), and D-AB-FeP (–•–).

spectra of ZnP and H_2P. The fluorescence spectra of the donors (D) are almost indistinguishable from the spectra of D-B (not shown), and the acceptor is nonfluorescent. It is clear that for both series of four D-B-A systems, the donor fluorescence is quenched, and that the smallest degree of quenching is found for the system with bicyclo[2.2.2]octane (OB) as the central unit in the bridging chromophore. The decrease in the fluorescence intensity and in the donor fluorescence lifetime were used to calculate the efficiency (E) and the total rate constant (k_{DBA}) for quenching of the donor singlet excited state in the D-B-A systems [Eq. (1)]

$$k_{DBA} = \frac{E}{(1-E)\tau_f^0} \qquad :E = 1 - \frac{F}{F_0} = 1 - \frac{\tau_f}{\tau_f^0} \tag{1}$$

F and F_0 are the total donor fluorescence intensities in the D-B-A systems and in the D-B references, respectively, and τ_f and τ_f^0 are the corresponding fluorescence lifetimes.

Since FeP is nonfluorescent, the donor lifetimes in D-B-A and in D-B were determined by using a single-exponential model in the analysis of the time-resolved data. The fluorescence lifetimes of the reference compounds were, within experimental error, independent of the bridging chromophore. The efficiencies calculated from steady-state and time-resolved measurements were the same (within 15%), and k_{DBA} was calculated from an average E value.[28] Both the steady-state and time-resolved measurements were performed in seven different solvents, and the calculated k_{DBA} values are compiled in Tables 1 and 2.

The results in Tables 1 and 2 indicate that the rate constant for quenching by the acceptor is affected by the change of electronic structure of the bridging chromophore, with the quenching rate constant increasing in the order D-OB-A < D-BB-A < D-NB-A < D-AB-A for both sets of systems. The change in quenching rate is not dramatic, and for the ZnP-RB-FeP systems it is in the range of $1-4\times10^9\ s^{-1}$, and for the H_2P-RB-FeP systems the quenching is an order of magnitude less, in the range of $1-7\times10^8\ s^{-1}$. It is also notable that the rate constants in our systems show essentially no solvent dependence. The total quenching rate constants observed for our ZnP/FeP systems are comparable to those previously reported for other rigid ZnP-bridge-FeP systems with similar donor–acceptor distances.[18, 33, 35]

Fluorescence, internal conversion, and intersystem crossing: The spectroscopic properties of D-B are very similar to those of D, regarding the fluorescence lifetime (τ_f^0), quantum yield (ϕ_f^0), and fluorescence and absorption spectra. Assuming that the quantum yield for triplet formation (ϕ_{isc}^0) is the same for diphenyl-substituted porphyrins as for tetraphenyl-substituted porphyrins, one can calculate the rate constant for

Table 1. The refractive index (n), dielectric constant (ε), calculated driving force (ΔG^0) and reorganization energy (λ), observed total rate constants (k_{DBA}[a]), and calculated Förster rate constants ($k_{Förster}$[b]) for ZnP-RB-FeP in different solvents at 20 °C.

Solvent	n[c]	ε[c]	ΔG^0 [eV]	λ [eV]	$\Delta G^0 + \lambda$ [eV]	ZnP-OB-FeP k_{DBA} [s^{-1}]	ZnP-BB-FeP k_{DBA} [s^{-1}]	ZnP-NB-FeP k_{DBA} [s^{-1}]	ZnP-AB-FeP k_{DBA} [s^{-1}]	ZnP/FeP $k_{Förster}$ [s^{-1}]
1,4-dioxane	1.422	2.219	−0.22	0.21	−0.01	$1.0\pm0.1\times10^9$	$1.5\pm0.2\times10^9$	$1.9\pm0.2\times10^9$	$2.7\pm0.5\times10^9$	$0.4\pm0.1\times10^9$
toluene	1.496	2.379	−0.30	0.16	−0.14	$1.1\pm0.1\times10^9$	$1.5\pm0.2\times10^9$	$1.8\pm0.2\times10^9$	$2.5\pm0.5\times10^9$	$0.4\pm0.1\times10^9$
$CHCl_3$	1.446	4.807	−0.82	0.76	−0.06	$1.0\pm0.1\times10^9$	$1.5\pm0.2\times10^9$	$2.0\pm0.2\times10^9$	$2.8\pm0.6\times10^9$	$0.3\pm0.1\times10^9$
THF	1.405	7.52	−0.98	1.01	+0.03	$1.0\pm0.1\times10^9$	$1.4\pm0.1\times10^9$	$1.9\pm0.2\times10^9$	$3.8\pm0.8\times10^9$	$0.5\pm0.1\times10^9$
CH_2Cl_2	1.424	8.93	−1.05	1.03	−0.02	$1.1\pm0.1\times10^9$	$1.7\pm0.2\times10^9$	$2.0\pm0.2\times10^9$	$4.2\pm0.8\times10^9$	$0.4\pm0.1\times10^9$
butanol	1.399	17.84	−1.16	1.21	+0.05	$0.7\pm0.1\times10^9$	$1.1\pm0.1\times10^9$	$1.7\pm0.2\times10^9$	$2.6\pm0.5\times10^9$	$0.2\pm0.1\times10^9$
DMF	1.431	38.25	−1.23	1.22	−0.01	$0.7\pm0.1\times10^9$	$1.3\pm0.1\times10^9$	$1.8\pm0.2\times10^9$	–[d]	$0.3\pm0.1\times10^9$

[a] Uncertainties based on differences in steady-state and lifetime measurements. [b] Uncertainties based on uncertainties in lifetime, quantum yield, and molar absorptivity. [c] From ref. [50]. [d] Not determined due to electron transfer from ZnP to AB in DMF (see ref. [59]).

Table 2. The refractive index (n), dielectric constant (ε), calculated driving force (ΔG^0) and reorganization energy (λ), observed total rate constants (k_{DBA}[a]), and calculated Förster rate constants ($k_{Förster}$[b]) for H_2P-RB-FeP in different solvents at 20 °C.

Solvent	n[c]	ε[c]	ΔG^0 [eV]	λ [eV]	$\Delta G^0 + \lambda$ [eV]	H_2P-OB-FeP k_{DBA} [s^{-1}]	H_2P-BB-FeP k_{DBA} [s^{-1}]	H_2P-NB-FeP k_{DBA} [s^{-1}]	H_2P-AB-FeP k_{DBA} [s^{-1}]	H_2P/FeP $k_{Förster}$ [s^{-1}]
1,4-dioxane	1.422	2.219	+0.13	0.21	+0.34	$1.6 \pm 0.3 \times 10^8$	$2.7 \pm 0.7 \times 10^8$	$3.4 \pm 0.9 \times 10^8$	$5.9 \pm 1.8 \times 10^8$	$0.5 \pm 0.1 \times 10^8$
toluene	1.496	2.379	+0.05	0.16	+0.21	$1.6 \pm 0.3 \times 10^8$	$3.1 \pm 0.8 \times 10^8$	$3.7 \pm 0.9 \times 10^8$	$5.6 \pm 1.7 \times 10^8$	$0.4 \pm 0.1 \times 10^8$
$CHCl_3$	1.446	4.807	−0.46	0.76	+0.30	$1.4 \pm 0.3 \times 10^8$	$2.8 \pm 0.7 \times 10^8$	$3.4 \pm 0.9 \times 10^8$	$6.3 \pm 1.9 \times 10^8$	$0.6 \pm 0.1 \times 10^8$
THF	1.405	7.52	−0.64	1.01	+0.37	$2.0 \pm 0.4 \times 10^8$	$3.2 \pm 0.8 \times 10^8$	$4.3 \pm 1.1 \times 10^8$	$6.6 \pm 2.0 \times 10^8$	$0.6 \pm 0.1 \times 10^8$
CH_2Cl_2	1.424	8.93	−0.69	1.03	+0.34	$1.2 \pm 0.2 \times 10^8$	$2.1 \pm 0.5 \times 10^8$	$2.6 \pm 0.7 \times 10^8$	$4.6 \pm 1.4 \times 10^8$	$0.6 \pm 0.1 \times 10^8$
butanol	1.399	17.84	−0.83	1.21	+0.38	$1.2 \pm 0.2 \times 10^8$	$1.5 \pm 0.4 \times 10^8$	$2.1 \pm 0.5 \times 10^8$	$3.6 \pm 1.1 \times 10^8$	$0.6 \pm 0.1 \times 10^8$
DMF	1.431	38.25	−0.90	1.22	+0.32	$2.4 \pm 0.5 \times 10^8$	$4.2 \pm 1.1 \times 10^8$	$4.0 \pm 1.0 \times 10^8$	$4.5 \pm 1.4 \times 10^8$	$0.4 \pm 0.1 \times 10^8$

[a] Uncertainties based on differences in steady-state and lifetime measurements. [b] Uncertainties based on uncertainties in lifetime, quantum yield, and molar absorptivity. [c] From ref. [50].

fluorescence (k_f^0), for non-radiative deactivation to the ground state (k_{ic}^0), and for triplet formation (k_{isc}^0) for the donor moieties (Scheme 1; the superscript "0" indicating the absence of acceptor). The quantum yields for intersystem crossing of free-base tetraphenylporphyrin (H_2TPP) and zinc porphyrin (ZnTPP) in polar solvents are 0.88 and 0.90, respectively.[43] For ZnP this gives $k_f^0 = \phi_f^0/\tau_f^0 \approx 2 \times 10^7\ s^{-1}$, $k_{isc}^0 = \phi_{isc}^0/\tau_f^0 \approx 6 \times 10^8\ s^{-1}$ yielding $k_{ic}^0 \approx 7 \times 10^7\ s^{-1}$, and the corresponding data for H_2P are $k_f^0 = \phi_f^0/\tau_f^0 \approx 5 \times 10^6\ s^{-1}$, $k_{isc}^0 = \phi_{isc}^0/\tau_f^0 \approx 8 \times 10^7\ s^{-1}$ yielding $k_{ic}^0 \approx 6 \times 10^6\ s^{-1}$. Assuming that the intrinsic rate constants for deactivation of the singlet excited donor state to the ground state do not change in the D-B-A systems, the quantum yield for intersystem crossing can be estimated by using nanosecond transient absorption. For ZnP-RB-FeP systems this was done by comparing the initial ΔA of ^{3}ZnP in ZnP-OB-FeP with that of ZnP-OB at 470 nm (Figure 5). The substitution pattern of the investigated

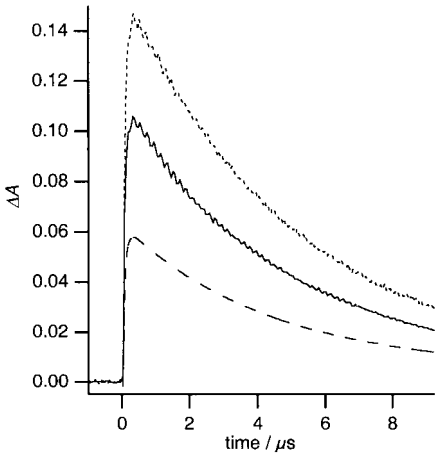

Figure 5. Kinetic traces ($\lambda_{pump} = 532$ nm, $\lambda_{probe} = 470$ nm) of ^{3}ZnP in ZnP-OB (••••), ZnP-OB-FeP (——), and the expected trace (- - - -) of ZnP-OB-FeP assuming $k_{isc} = k_{isc}^0$.

porphyrins results in a nonplanar ring conformation in the triplet excited state that in turn leads to an unusual fast decay to the ground state for both ZnP and H_2P samples.[44] The decay times of the ZnP triplet state in ZnP-OB-FeP and ZnP-OB are approximately equal (≈ 5 μs), indicating that the donor triplet state is not significantly quenched by the acceptor. This is in agreement with investigations of ZnP-OB-H_2P, which does not exhibit any triplet energy transfer from ZnP to H_2P.[45] In Figure 5, the expected kinetic trace of ZnP-OB-FeP is also shown. It has been constructed assuming that the rates of intersystem crossing are equal in ZnP-OB and ZnP-OB-FeP, that is, assuming the acceptor has no effect on the intersystem-crossing rate. In this case, the expected ϕ_{isc} in the ZnP-OB-FeP system can be calculated as $k_{isc}^0 \times \tau_f = 0.35$, where τ_f is the fluorescence lifetime of the donor in the D-B-A system. In contrast, the quantum yield determined by comparison of the initial ΔA's is $\phi_{isc} = \Delta A_{DBA}/\Delta A_{DB} \times \phi_{isc}^0 = 0.67$. The difference suggests an increase in the rate constant for intersystem crossing from $k_{isc}^0 = 6 \pm 1 \times 10^8\ s^{-1}$ to $k_{isc} = 11 \pm 2 \times 10^8\ s^{-1}$ due to the presence of FeP. The same proportional increase in k_{isc} was found for the H_2P-OB-FeP system, and, again, the decays of ^3H_2P in H_2P-OB and H_2P-OB-FeP were found to be the same (≈ 10 μs). The measured and expected quantum yields were 0.49 and 0.26, respectively, giving an increase from $k_{isc}^0 = 8 \pm 1 \times 10^7\ s^{-1}$ to $k_{isc} = 16 \pm 2 \times 10^7\ s^{-1}$. The reliability of the method can be estimated from measurements of the ZnP-OB-H_2P system, which gave a calculated quantum yield of 0.59 and a measured quantum yield of 0.67, corresponding to $k_{isc}^0 = 6 \times 10^8\ s^{-1}$ and $k_{isc} = 7 \times 10^8\ s^{-1}$, respectively.

Förster theory for energy transfer: In the systems investigated, long-range energy transfer from ZnP or H_2P to FeP is thermodynamically favorable. For systems with D–A distances >10 Å, Förster theory can be expected to adequately describe the direct donor–acceptor energy transfer, neglecting any influence from the bridge.[46, 47] The expected Förster energy transfer rate constant ($k_{Förster}$) can be estimated from the photophysical properties of the separate donor and acceptor moieties [Eq. (2)].

$$k_{Förster} = 8.79 \times 10^{-25} \frac{\phi_f^0 \kappa^2 J}{\tau_f^0 n^4 R^6} \quad (2)$$

The orientation factor (κ^2) depends on the orientation of the donor and acceptor transition dipoles.[48] We expect the transition dipoles of both ZnP and FeP to be degenerate in the porphyrin plane,[28, 49] and since the planes are almost freely rotating with respect to each other, the average $\kappa^2 = 2/3$ for random orientation can be used. For H_2P the transition dipoles are directed along the N–N axes (making a 45° angle with the porphyrin connecting axis), which changes the orientation factor to $\kappa^2 = 5/6$.[28, 48] The donor–acceptor center-to-center distance ($R = 25.3$ Å; estimated by molecular

0947-6539/01/0710-2126 $ 17.50+.50/0 *Chem. Eur. J.* **2001**, *7*, No. 10

mechanics) is the same for all D-B-A systems. n is the refractive index of the solvents used,[50] and ϕ_f^0 and τ_f^0 are the fluorescence quantum yield and lifetime, respectively, of the donor in the absence of the acceptor. The spectral overlap integral, J, is calculated from the acceptor absorption spectrum ($\varepsilon(\lambda)$) and the normalized donor fluorescence spectrum ($F(\lambda)$) [Eq. (3)].

$$J = \int_0^\infty \varepsilon(\lambda) F(\lambda) \lambda^4 \mathrm{d}\lambda \tag{3}$$

The rate constants for the calculated Förster energy transfer in the ZnP-RB-FeP systems varies between 0.2–$0.5 \times 10^9\ s^{-1}$, depending on the solvent, and between 0.4–$0.6 \times 10^8\ s^{-1}$ for the H_2P-RB-FeP systems (Tables 1 and 2).

Marcus theory for electron transfer: The generally accepted theory for diabatic electron transfer (ET) is that of Marcus, which relates the rate constant for electron transfer (k_{ET}) to the electronic coupling (V), the driving force (ΔG^0) for the reaction, and the reorganization energy (λ) due to structure (λ_i) and solvent (λ_s). If V is small relative to λ and the energy of the promoting vibration, the rate constant is given by Equation (4):[51–53]

$$k_{ET} = \sqrt{\frac{\pi}{\hbar^2 \lambda k_B T}} |V|^2 \exp\left(\frac{-(\Delta G^0 + \lambda)^2}{4\lambda k_B T}\right) \tag{4}$$

As a result of the quadratic form of $(\Delta G^0 + \lambda)$, this expression leads to both a normal region in which k_{ET} increases with more negative ΔG^0, as well as an inverted region where k_{ET} decreases with more negative ΔG^0 after the maximum in k_{ET} is reached at $-\Delta G^0 = \lambda$.

According to Equation (4), k_{ET} depends, in addition to the electronic coupling, upon the driving force and reorganization energy. ΔG^0 and λ can be calculated from the donor/acceptor redox potentials (E_{ox} and E_{red}), the 0–0 excitation energy of the donor (E_{00}), the donor-acceptor distance (R_{DA}) and radii of donor and acceptor (R_D, R_A), and finally the dielectric constant (ε_s) and refractive index of the solvent (n) used in the ET measurements, together with the dielectric constant of the solvent used in the electrochemical measurements (ε_s^{ref}) [Eqs. (5) and (6)]:[54–58]

$$\Delta G^0 = e(E_{ox} - E_{red}) - E_{00} - \frac{e^2}{4\pi\varepsilon_0\varepsilon_s R_{DA}} + \frac{e^2}{4\pi\varepsilon_0}\left(\frac{1}{\varepsilon_s} - \frac{1}{\varepsilon_s^{ref}}\right)\left(\frac{1}{2R_D} + \frac{1}{2R_A}\right) \tag{5}$$

$$\lambda = \lambda_i + \lambda_s = \lambda_i + \frac{e^2}{4\pi\varepsilon_0}\left(\frac{1}{2R_D} + \frac{1}{2R_A} - \frac{1}{2R_{DA}}\right)\left(\frac{1}{n^2} - \frac{1}{\varepsilon_s}\right) \tag{6}$$

The redox potentials of H_2P, ZnP, and FeP were determined in CH_2Cl_2 by cyclic voltammetry [H_2P: $E_{ox} = 0.56$ V, ZnP: $E_{ox} = 0.38$ V, FeP: $E_{red} = -0.72$ V vs Ag/Ag^+ electrode (10 mM in acetonitrile, $E = 0.45$ V vs SHE)],[59] and are in fair agreement with other reported data for etio- and tetraphenylporphyrins.[60] By using these redox potentials, $E_{00} = 2.12$–2.15 eV for ZnP (depending upon solvent) and $E_{00} = 1.97$ eV for H_2P, $R_D = R_A = 4.8$ Å, $\lambda_I = 0.1$ eV,[22] and the appropriate solvent properties, ΔG^0 and λ were calculated and the results are summarized in Tables 1 and 2. Since negative ΔG^0 values were determined for both systems in most solvents, electron transfer should be thermodynamically favorable. Furthermore, for the ZnP-RB-FeP systems (Table 1), $-\Delta G^0 \approx \lambda$ in all solvents and, therefore, these systems are expected to show the maximum rate constant for electron transfer without solvent dependence. For the H_2P-RB-FeP systems (Table 2), however, the donor oxidation potential is higher, so electron transfer should be in the normal region ($-\Delta G^0 < \lambda$), resulting in a slower rate.

Electronic coupling: In order to predict the rate constant for ET from Marcus theory [Eq. (4)], the value of the coupling constant is needed. We have estimated a value for the electronic orbital coupling between the porphyrin moieties by a method introduced by Larsson.[61, 62] The electronic coupling was calculated for ZnP-RB-ZnP systems, which are structurally identical to the ZnP-RB-FeP and H_2P-RB-FeP systems studied. By using symmetric structures we may take the energy difference between $LUMO = \psi_{left} + \psi_{right}$ and $LUMO^{\#} = \psi_{left} - \psi_{right}$ (ψ_{left} and ψ_{right} are LUMOs on the left and right porphyrin, respectively). The influence of the bridging chromophores on V is found indirectly from the effect it has on the energy gap between the near-degenerate LUMO and LUMO$^{\#}$. The minimum energy gap between LUMO and LUMO$^{\#}$ is calculated by perturbing the system by a point charge (in our case H_3O^+), which forms the reaction field necessary to reach the point of avoided crossing between the energy curves of the porphyrin moieties. At this point, the smallest LUMO/LUMO$^{\#}$ energy splitting appears when LUMO and LUMO$^{\#}$ are distributed equally between the porphyrin moieties. The coupling element for photoinduced electron transfer can then be calculated, using Koopmans' theorem, as $V = (E_{LUMO^{\#}} - E_{LUMO})/2$. The calculations were performed for a selected range of conformations by changing the dihedral angle (ω) between the porphyrin and adjacent phenyl group and the orientation (φ) of the central unit relative to the porphyrin planes (Figure 6). The electronic couplings for the different conformations were averaged and statistically weighted according to the Boltzmann distribution of the conformations.[28] In the systems containing conjugated bridging chromophores (BB, NB, AB), the electronic coupling was dependent on the orientation of the central unit with respect to the phenyl groups. Maximum coupling was found when the central unit was coplanar with the phenyl groups, and the coupling followed a $\cos^2$ dependence to the minimum (zero) coupling, which was found when the central unit was perpendicular to the plane of the phenyl groups. Furthermore, the coupling was dependent on the dihedral angle (ω) between the porphyrin moiety and the connected phenyl group in all systems. For perpendicular phenyl and porphyrin planes ($\omega = 90°$), the coupling is zero, but as ω is changed towards a more planar porphyrin/phenyl conformation, the coupling increases. The average V from a Boltzmann distribution of the different conformations at room temperature is 0.05, 2.2, 3.5, and 8.1 cm^{-1} for the systems with OB, BB, NB, and AB bridging chromophores, respectively. According to the Marcus equation [Eq. (4)], these average electronic couplings result in electron transfer rates of approximately $7 \times 10^5\ s^{-1}$, $1 \times 10^9\ s^{-1}$, $3 \times 10^9\ s^{-1}$, and $2 \times 10^{10}\ s^{-1}$, respectively, for the ZnP-RB-FeP systems.

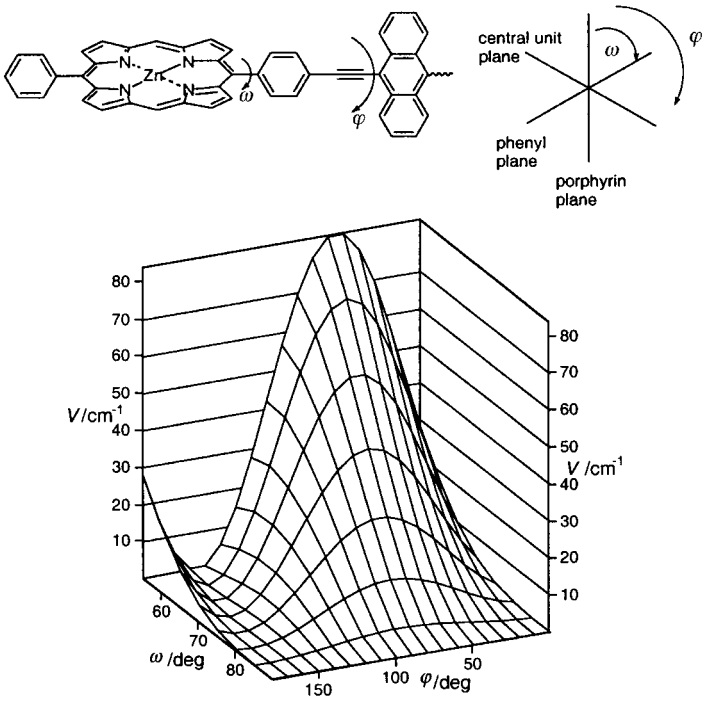

Figure 6. Plot of the variation in the calculated electronic coupling constant (V) with the dihedral angles (ω and φ) for the ZnP-AB-ZnP system.

Detecting the ZnP radical cation, ZnP$^{\bullet+}$: Although the calculations suggest electron transfer to be feasible, the only direct proof of the occurrence of ET lies in the detection of the charge-separated state. Transient absorption measurements of ZnP-AB and ZnP-AB-FeP in a highly polar solvent (DMF) have shown that fast ($\approx 4 \times 10^{10}\ s^{-1}$) electron transfer ZnP → AB occurs, along with stepwise electron transfer, ZnP → AB → FeP.[59] Figure 7 shows the transient absorption

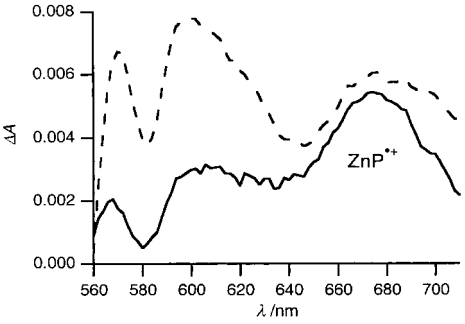

Figure 7. Transient absorption spectra of ZnP-NB-FeP (– – –) and ZnP-AB-FeP (——, scaled ×2) at 1.6 ns in DMF ($\lambda_{pump} = 545$ nm).

spectra of ZnP-NB-FeP and ZnP-AB-FeP in DMF at 1.6 ns. We chose this solvent because ET is most likely to occur in a solvent of high polarity. For ZnP-NB-FeP, bleaching/stimulated emission features are superimposed on the broad absorption of the ZnP excited singlet state, and there is no clear positive peak at 680 nm. In contrast, no stimulated emission at about 645 nm is observed for ZnP-AB-FeP, and we assign the clearly visible peak at 680 nm to the ZnP$^{\bullet+}$ radical cation.[16, 63, 64] This spectral feature is observed in solutions of both ZnP-AB-FeP and ZnP-AB in DMF. The kinetics differ significantly though, with fast forward ($\approx$20 ps) and back ($\approx$50 ps) transfer in ZnP-AB, but a long-lived nanosecond transient is detected for ZnP-AB-FeP. This has been interpreted as a stepwise charge separation, ZnP → AB → FeP, followed by a slow recombination reaction, FeP → ZnP.[59]

However, in the other bridged systems, ZnP-RB-FeP (R = O, B, N), no ZnP$^{\bullet+}$ peak was observed, as shown for ZnP-NB-FeP in Figure 7, indicating that long-range ET is *not* an important deactivation process of the singlet excited donor. In addition, no ZnP$^{\bullet+}$ signal was detected for ZnP-AB-FeP in solvents with lower polarity than DMF. The transient absorption spectra of all compounds in which the ZnP$^{\bullet+}$ peak was not detected are essentially the same as the spectrum of ZnP-NB-FeP shown in Figure 7. By simulating the ^{1}ZnP*-AB-FeP → ZnP$^{\bullet+}$-AB-FeP$^{\bullet-}$ → ZnP-AB-FeP reaction and comparing with the efficiency for the step-wise process,[59] we find that for $k_{ET} < 2 \times 10^8\ s^{-1}$, the population of ZnP$^{\bullet+}$ would most likely be too small to detect. This rate was estimated by assuming that the recombination rate of $< 2 \times 10^8\ s^{-1}$, observed for ZnP$^{\bullet+}$-AB-FeP$^{\bullet-}$ in DMF, is independent of the bridging chromophore and solvent.

Temperature effects: The temperature dependence of the quenching of the excited singlet state of the donor was measured in 2-methyl-THF in the temperature range 300–100 K. The largest temperature dependence was observed for systems that contained AB as the bridging chromophore, and a decrease in k_{DBA} with decreasing temperature was observed. Only minor temperature effects were found for the other systems, with sensitivity to temperature decreasing from NB to BB to OB (Figure 8). This behavior is very similar to what was observed for the corresponding systems showing only energy transfer (ZnP-RB-H_2P).[65]

Discussion

Donor–acceptor systems based on porphyrin moieties have been extensively studied. In most cases it has been argued that in systems containing ZnP and FeP, the major mechanism leading to quenching of donor fluorescence over a wide range of donor-acceptor distances is photoinduced electron transfer.[16, 18, 21, 32–35] In these previously investigated systems, the center-to-center distance between donor and acceptor varies from approximately 10 to 40 Å. In the systems investigated here we intended to study the effect of the bridging chromophore on electron transfer. However, since we failed to detect the charge-separated state, we decided to investigate all likely pathways (Scheme 1) for the deactivation of the singlet excited donor state on an equal footing. The porphyrin systems investigated were all geometrically similar, but the electronic properties of the bridging chromophore varied. Furthermore, we also investigated the effect of changing the donor porphyrin to H_2P in a similar series. In all our systems, the D–A distance was kept constant at 25 Å. Based on the finding that the absorption spectra of the D-B-A systems do

  0947-6539/01/0710-2128 $ 17.50+.50/0 *Chem. Eur. J.* **2001**, *7*, No. 10

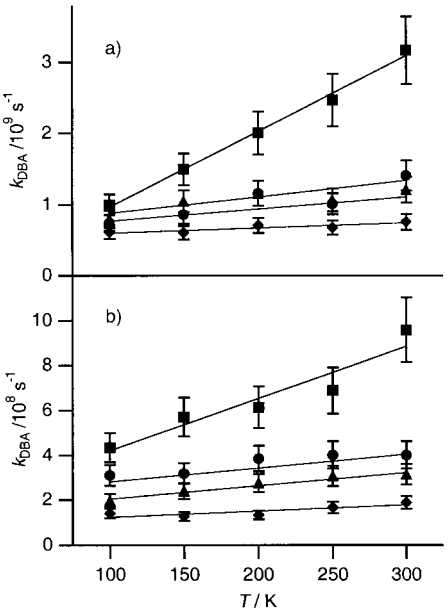

Figure 8. Temperature dependence of k_{DBA}. a) D = ZnP, b) D = H_2P: D-OB-FeP (◆), D-BB-FeP (▲), D-NB-FeP (●), and D-AB-FeP (■) (guiding lines (——)).

not significantly differ from a spectral sum of D, B, and A, we consider the systems to be composed of three discrete chromophores.

For both series, ZnP-RB-FeP and H_2P-RB-FeP, the fluorescence of the donor was quenched in all the D-B-A systems relative to the D-B references. The extent of quenching followed the order D-AB-A > D-NB-A > D-BB-A > D-OB-A for both series, but the differences between the bridging chromophores were not very large. In previous studies of ZnP-RB-H_2P systems that indicated only donor energy transfer quenching,[28] the bridging chromophore was shown to play a considerable mediating role, with the effect being proportional to the inverse energy gap between donor and bridge excited states. The smaller differences between the bridging chromophores observed in the FeP-containing systems suggests that energy transfer may not be the only quenching process. The energy-transfer rates calculated by using Förster theory were on the order of $4 \times 10^8\ s^{-1}$ for the ZnP-RB-FeP systems and $6 \times 10^7\ s^{-1}$ for the H_2P-RB-FeP systems. Simple Förster theory takes into account only the dipolar properties of the donor and acceptor, and considers the bridge to be an electronically inert spacer. However, as mentioned above, we have previously demonstrated that the bridging chromophores do have a mediating effect on the energy transfer, and that the constant (k_{EET}) can be written as a sum of $k_{mediating}$ and $k_{Förster}$.

Unfortunately, the mediating effect cannot be measured directly in the systems investigated here, because, besides energy transfer, there are additional deactivation pathways. This being the case, it seems reasonable to use the $k_{mediating}$ calculated for the ZnP-RB-H_2P systems previously investigated (Table 3), because the bridging chromophores, conformational restrictions, and D – A distances are the same as in the present ZnP-RB-FeP systems. In particular, an identical D – A distance is important, since the dependence of $k_{Förster}$ on

Table 3. The average rate constants for additional deactivation pathways of the singlet excited donor state in the D-B-A systems. k' is the remaining rate constant calculated as $k_{DBA} - \Sigma k_{other}$.

Compound	k_{DBA} [s^{-1}]	$k_{isc} - k^0_{isc}$ [s^{-1}]	$k_{Förster}$ [s^{-1}]	$k_{mediating}$ [s^{-1}]	k' [s^{-1}][a]
ZnP-OB-FeP	0.9×10^9	0.5×10^9	0.4×10^9	0.05×10^9	0
ZnP-BB-FeP	1.4×10^9	$\geq 0.5 \times 10^9$	0.4×10^9	0.17×10^9	0.3×10^9
ZnP-NB-FeP	1.9×10^9	$\geq 0.5 \times 10^9$	0.4×10^9	0.22×10^9	0.8×10^9
ZnP-AB-FeP	3.1×10^9	$\geq 0.5 \times 10^9$	0.4×10^9	0.87×10^9	1.3×10^9
H_2P-OB-FeP	1.6×10^8	0.8×10^8	0.6×10^8	$< 0.5 \times 10^8$	0
H_2P-BB-FeP	2.8×10^8	$\geq 0.8 \times 10^8$	0.6×10^8	$< 1.7 \times 10^8$	0
H_2P-NB-FeP	3.4×10^8	$\geq 0.8 \times 10^8$	0.6×10^8	$< 2.2 \times 10^8$	0
H_2P-AB-FeP	5.3×10^8	$\geq 0.8 \times 10^8$	0.6×10^8	$< 8.7 \times 10^8$	0

[a] Negative k' is reported as 0 and is due to the uncertainty in all determined rate constants.

the distance is proportional to R^6 and $k_{mediating}$ is also likely to be distance dependent. In systems devised for the investigation of distance dependence, it is therefore necessary to take into account energy transfer as a likely deactivation pathway. For the systems with H_2P instead of ZnP as the donor, we expect that the mediation will be smaller, but of the same order of magnitude, since both donors have similar excitation energies (ZnP $\approx 17\,400\ cm^{-1}$, $H_2P \approx 16\,000\ cm^{-1}$) and, hence, similar donor-bridge energy gaps. We anticipate that the change of donor will have the largest effect on the mediation through AB, since this bridge is closest in energy to the donor.

It is apparent from both triplet yields (ϕ^0_{isc}) and estimated intramolecular deactivation rate constants (k^0_f, k^0_{ic}, k^0_{isc}) of the donor porphyrins, that the dominant singlet-state decay pathway is triplet state formation. Furthermore, in the D-B-A systems containing a paramagnetic high-spin iron(III) chloride porphyrin, the rate constant for intersystem crossing is almost doubled, regardless of which of the two donors is present. Enhanced triplet formation has previously been observed in systems that contain other paramagnetic species, such as copper porphyrins.[30, 31, 66] In the task of dividing the total rate constant for the donor quenching (k_{DBA}) into the different pathways, the enhancement of k_{isc} when the acceptor is present is the only intramolecular quenching pathway listed in Table 3. The enhancement of k_{isc} was determined in the systems with the nonconjugated bridging chromophore (OB), since in these systems triplet energy transfer does not occur. It is important to note that the reported increase in k_{isc} is thus the *minimum* value for the series, and the effect of FeP on the intersystem crossing of the donor porphyrin might very well be stronger in the systems having conjugated bridging chromophores.

By measuring the total rate of quenching, and estimating the rate constants of enhanced intersystem crossing and bridge-mediated singlet energy transfer, it is possible to calculate rate constants for the remaining pathways: $k' = k_{DBA} - \Sigma k_{other}$. Such data are shown in Table 3, where it is evident that for all the H_2P-RB-FeP systems, the directly observed processes account for the quenching. This is also the case for ZnP-OB-FeP, but for ZnP-BB-FeP, ZnP-NB-FeP, and ZnP-AB-FeP, 20 – 40 % of k_{DBA} is left unaccounted for. Photoinduced electron transfer is a (thermodynamically) possible quenching pathway, but since no $ZnP^{\bullet+}$ signal was

observed by transient absorption, we were able to estimate the maximum rate of ET to be less than $2 \times 10^8\ s^{-1}$, as charge separation faster than this should give a detectable signal. This indicates that ET plays only a minor role in the donor deactivation, and the remaining k' may be attributed to the uncertainty in k_{isc} in the systems with conjugated bridging chromophores. By the use of transient absorption, ET has previously been shown to occur in ZnP/FeP systems, albeit with shorter D – A distances.[16, 32, 34] This suggests that the rather long distance (25 Å center-to-center, 19 Å edge-to-edge) in the systems investigated here is the reason why electron transfer does not occur. In systems with shorter D – A distances, the electronic coupling for electron transfer is probably large enough for k_{ET} to dominate over k_{EET}, making electron transfer the major deactivation pathway. Our findings of enhanced intersystem crossing and energy transfer as major deactivation pathways agree with an early study of flexible ZnP/FeP systems by Brookfield et al.[66]

One further indication that electron transfer plays only a minor role in the investigated systems is that the quenching is independent of solvent polarity in both series. The solvents were chosen on the basis of D-B-A solubility and differences in polarity. We note that butanol may not be a suitable choice of solvent for systems containing FeP, since it has been shown that FeP reacts with alcohols to form a radical species.[67] However, the quenching results obtained in butanol do not differ significantly from those obtained in the other six solvents. According to Marcus theory for electron transfer, k_{ET} is dependent upon the driving force (ΔG^0) and solvent reorganization energy (λ_s), which are both a function of solvent polarity. It may therefore be expected that k_{ET} will change with solvent and, in the normal region, an increase in rate constant with increasing solvent polarity should be the result. When $-\Delta G^0 \approx \lambda$, no solvent dependence is expected. The calculations of these parameters for the ZnP-RB-FeP series suggest that these systems fall into this region and thus the rate of electron transfer will then be thermodynamically optimal. However, for the H_2P-RB-FeP series normal region behavior is predicted, because the higher oxidation potential and lower excitation energy of the donor effectively add 0.3 eV to ΔG^0. Although it may be argued that parameters such as radii and internal reorganization energy used in the Marcus theory are only crude estimates, it is unlikely that they are very different in the two series with ZnP or H_2P as the donor. Thus, if electron transfer is a major deactivation pathway, at least one of the series should exhibit a marked solvent dependence of the rate constant.

Using Marcus theory to calculate the rate for electron transfer, requires estimates of several parameters. The D – A distance (R_{DA}) can be obtained from molecular modeling or quantum mechanical calculations, and the radii of donor (R_D) and acceptor (R_A) can be found either from quantum mechanical calculations, or taken from other investigations of electron transfer in porphyrin-based systems. We chose the latter approach, using values for the radii and internal reorganization energy (λ_i) based on electron-transfer properties of similar porphyrin systems.[22] The driving force (ΔG^0) and solvent reorganization energy (λ_s) were calculated from the above-mentioned parameters, the solvent properties, and from experimental measurements. The final parameter, the electronic coupling (V), which controls the "communication" between the donor and acceptor, has previously been modeled in many ways,[15, 68] but we chose a quantum mechanical approach that estimates V from the LUMO/LUMO$^{\#}$ energy gap in systems perturbed to reach the point of avoided crossing for the chromophore potential-energy curves.[62] Calculations on ZnP-RB-ZnP show that porphyrins with conjugated bridging chromophores should be able to couple electronically, but that there are large differences between the bridging chromophores, following the trend AB $\gg$ NB $>$ BB. Since we did not detect the charge-separated state for any of the systems, the true electronic coupling for electron transfer must be much smaller than calculated and is probably less than $1\ cm^{-1}$. In the method we used for calculating V, errors arise from the neglect of the extensive configuration interaction in the S_1 state as well as in the lowest charge-transfer states of the porphyrins. This probably lowers the calculated coupling. Furthermore, for convenience, ZnP was used as both donor and acceptor in the calculations. This might account for some of the discrepancy between the experimental results and the electron-transfer rates predicted from the calculations, since in the reduced form of ZnP, it is believed that the charge is located on the ring system, whereas the reduction of FeP takes place at the metal center.[60] Furthermore, FeP with chloride as counter ion is a high-spin complex, that is, it is not a singlet in the excited state, and the absorption spectra of ZnP and FeP are very different. Therefore, the calculation of V can be expected to be more reliable for a system in which the acceptor is more closely comparable to ZnP. The corresponding gold porphyrin (AuP) is, in terms of spectra and ring reduction, a suitable candidate and the ZnP-RB-AuP systems have been prepared. In these systems we have shown that electron transfer can occur from the singlet excited ZnP.[69]

Conclusion

The investigated systems have equal donor/acceptor distances (25 Å), but the electronic structure of the bridging chromophore are varied. While it is likely that electron transfer is efficient in shorter systems, and that the electronic structure of the donor/acceptor intervening medium can enhance electron transfer, a charge-separated state was not observed in the systems studied in this work. However, as previously argued it is important to take into account other possible pathways for the quenching of the donor singlet excited state,[66] even when photoinduced electron transfer in donor-bridge-acceptor systems is predicted to be thermodynamically favorable. In summary, fluorescence quenching in itself should not be regarded as evidence for electron transfer, unless the charge-separated state can also clearly be detected.

In systems containing a paramagnetic porphyrin, the intersystem crossing rate in neighboring chromophores may be greatly enhanced. We have shown that the enhancement can easily be as large as 100%, and it might, therefore, contribute significantly to any observed decrease in donor fluorescence when comparing systems with and without the

  0947-6539/01/0710-2130 $ 17.50+.50/0 *Chem. Eur. J.* **2001**, *7*, No. 10

paramagnetic porphyrin. In donor–acceptor systems in which donor fluorescence and acceptor absorbance overlap, excitation energy transfer is also possible and it is important to know in detail what parameters influence energy transfer. Of special concern is the influence of the intervening medium.

Experimental Section

Synthesis of D-B-A systems and reference compounds: The synthesis of ZnP, H_2P, the donor reference compounds (ZnP-RB and H_2P-RB), and the ZnP-RB-H_2P systems have been described elsewhere.[28, 38]

Materials: Toluene and tetrahydrofuran (THF) were dried by distillation from sodium/benzophenone under nitrogen and used immediately after distillation. Commercially available reagents were purchased from Aldrich and used without further purification.

Methods: Column chromatography of iron porphyrins and ZnP-RB-FeP dimers was performed over silica gel (Merck, grade 60, 70—230 mesh) or aluminum oxide (activated, neutral, approx. 150 mesh) deactivated by addition of water to Brockmann grade III or IV. Proton (400 MHz) NMR spectra were recorded at room temperature with $CDCl_3$ as a solvent, using a Varian UNITY-400 NMR spectrometer. Chemical shifts are reported relative to tetramethylsilane ($\delta_H = 0$). Mass spectra were recorded by using a VG ZabSpec instrument. The substances were analyzed by positive FAB-MS (matrix: 3-nitrobenzyl alcohol) and high-resolution FAB-MS (HRMS) was performed with PEG 1000 as an internal standard. Deaeration of reaction mixtures was achieved by bubbling argon through the solution for 30 minutes. Iron insertion reactions were performed under argon.

Iron(III) 5,15-bis(3,5-di-*tert*-butylphenyl)-2,8,12,18-tetraethyl-3,7,13,17-tetramethylporphyrin chloride (FeP): Iron(II) bromide (98%, 50 mg, 0.23 mmol) was added to a deaerated solution of 5,15-bis(3,5-di-*tert*-butylphenyl)-2,8,12,18-tetraethyl-3,7,13,17-tetramethylporphyrin (H_2P, 24 mg, 28 μmol) in a 1:1 mixture of toluene and THF (20 mL) also containing collidine (0.1 mL). The reaction mixture was heated to reflux for 1 h. The solvents were removed under reduced pressure, and the residue was redissolved in CH_2Cl_2 (50 mL). The organic phase was washed with 10% HCl (4 × 20 mL), dried (Na_2SO_4), and evaporated. The crude product was added to an alumina column (grade III, 3 × 6 cm), and the iron porphyrin was eluted with CH_2Cl_2 leaving a bluish byproduct on the column. To ensure that the ferric chloride form was obtained, the product was dissolved in CH_2Cl_2, washed with saturated NaCl in 0.1 M HCl (2 × 30 mL), and dried over oven-dried NaCl. The solvent was removed in vacuo, and the iron(III) chloride porphyrin was recrystallized from CH_2Cl_2/hexane. Filtration gave 16 mg (60%) of FeP. HRMS calcd for $C_{60}H_{76}N_4Fe$ $[M-Cl]^+$: 908.542; found 908.547; UV/Vis ($CHCl_3$): $\lambda_{max} = 391$, 510, 648 nm.

FeP-RB: The free-base porphyrins H_2P-RB were converted to the corresponding iron(III) porphyrin chlorides using the same procedure as described for FeP.

FeP-OB: Yield 49%; HRMS calcd for $C_{70}H_{76}N_4Fe$ $[M-Cl]^+$: 1028.542; found 1028.548; UV/Vis ($CHCl_3$): $\lambda_{max} = 391$, 510, 648 nm.

FeP-BB: Yield 55%; HRMS calcd for $C_{68}H_{68}N_4Fe$ $[M-Cl]^+$: 996.480; found 996.487; UV/Vis ($CHCl_3$): $\lambda_{max} = 391$, 510, 648 nm.

FeP-NB: Yield 59%; HRMS calcd for $C_{72}H_{70}N_4Fe$ $[M-Cl]^+$: 1046.495; found 1046.495; UV/Vis ($CHCl_3$): $\lambda_{max} = 394$, 510, 648 nm.

FeP-AB: Yield 23%; FAB-MS calcd for $C_{76}H_{72}N_4Fe$ $[M-Cl]^+$: 1096.51; found 1096.54; UV/Vis ($CHCl_3$): $\lambda_{max} = 391$, 468, 648 nm.

ZnP-RB-FeP: The ZnP-RB-FeP dimers were prepared according to the procedure described here for ZnP-NB-FeP: Iron(II) chloride (99.998%, 5 mg, 39 μmol) was added to a deaerated solution of ZnP-NB-H_2P (12 mg, 7 μmol) in THF (20 mL) also containing collidine (0.1 mL). The reaction mixture was heated to reflux with an oil bath for approximately 1 h. TLC (SiO_2, 1% MeOH/$CHCl_3$) was used to monitor the reaction, which was stopped when the starting material ($R_f = 0.9$) was consumed. The solvent was removed under reduced pressure, and the residue was redissolved in CH_2Cl_2 (30 mL). The organic phase was washed with saturated aqueous NH_4Cl (2 × 25 mL) and brine (25 mL), dried (Na_2SO_4), and evaporated. The crude product was purified from a bluish byproduct by chromatography on alumina (grade III, 2 × 5 cm). The ZnP-NB-FeP dimer came off the column as a broad band eluting with CH_2Cl_2. A second fraction containing a mixture of the byproduct and residual ZnP-NB-FeP dimer was eluted with 1% MeOH/CH_2Cl_2 and was purified further using alumina grade IV (2 × 7 cm) and eluting with CH_2Cl_2. Traces of starting material (ZnP-NB-H_2P) were removed from the ZnP-NB-FeP dimer by chromatography (silica, 2 × 10 cm, $CHCl_3$ containing ca. 1% of EtOH as stabilizer). The free-base derivative eluted with the solvent front, whereas the product eluted slowly.

Zinc insertion was performed as a precaution to exclude the possibility of any H_2P-NB-FeP dimer present in the final product. Zinc acetate dihydrate (10 mg, 46 μmol) dissolved in MeOH (1 mL) was added to a solution of the dimer in CH_2Cl_2 (5 mL). The reaction mixture was stirred at room temperature for 1 h and diluted with EtOAc (30 mL). The organic phase was washed with 5% aqueous $NaHCO_3$ (25 mL), saturated aqueous NH_4Cl (2 × 25 mL), and brine (25 mL), dried (Na_2SO_4), and evaporated. Recrystallization of ZnP-NB-FeP from CH_2Cl_2/hexane afforded 6 mg (44%). FAB-MS calcd for $C_{118}H_{124}N_8FeZn$ $[M-Cl]^+$: 1772.9; found 1772.7; UV/Vis ($CHCl_3$): $\lambda_{max} = 411$, 538, 574 nm.

ZnP-OB-FeP: Yield 37%; FAB-MS calcd for $C_{116}H_{130}N_8FeZn$ $[M-Cl]^+$: 1754.9; found 1754.9; UV/Vis ($CHCl_3$): $\lambda_{max} = 412$, 538, 574 nm.

ZnP-BB-FeP: Yield 41%; FAB-MS calcd for $C_{114}H_{122}N_8FeZn$ $[M-Cl]^+$: 1722.8; found 1722.8; UV/Vis ($CHCl_3$): $\lambda_{max} = 414$, 538, 574 nm.

ZnP-AB-FeP: Yield 46%; FAB-MS calcd for $C_{122}H_{126}N_8FeZn$ $[M-Cl]^+$: 1822.9; found 1822.9; UV/Vis ($CHCl_3$): $\lambda_{max} = 410$, 450, 477, 538, 574 nm.

H_2P-RB-FeP: A sample of the ZnP-RB-FeP dimer, approximately 1 mg, was dissolved in CH_2Cl_2, and the solution was washed with 10% HCl, several portions of NH_4Cl/NH_3 buffer, and brine. The organic phase was dried over oven-dried NaCl, filtered, and evaporated. The zinc-porphyrin part of the dimer was quantitatively demetalated by using this procedure according to fluorescence measurements and FAB-MS.

H_2P-OB-FeP: FAB-MS calcd for $C_{116}H_{132}N_8Fe$ $[M-Cl]^+$: 1693.0; found 1692.9; UV/Vis ($CHCl_3$): $\lambda_{max} = 413$, 508, 542, 574 nm.

H_2P-BB-FeP: FAB-MS calcd for $C_{114}H_{124}N_8Fe$ $[M-Cl]^+$: 1660.9; found 1660.6; UV/Vis ($CHCl_3$): $\lambda_{max} = 412$, 508, 542, 574 nm.

H_2P-NB-FeP: FAB-MS calcd for $C_{118}H_{126}N_8Fe$ $[M-Cl]^+$: 1710.9; found 1710.8; UV/Vis ($CHCl_3$): $\lambda_{max} = 413$, 508, 542, 574 nm.

H_2P-AB-FeP: FAB-MS calcd for $C_{122}H_{128}N_8Fe$ $[M-Cl]^+$: 1761.0; found 1760.7; UV/Vis ($CHCl_3$): $\lambda_{max} = 410$, 476, 450, 506, 542, 574 nm.

The H_2P-containing compounds prepared by the method described above were used in all kinetic measurements. To record the absorption and steady-state fluorescence spectra, H_2P-containing compounds (H_2P-RB-FeP and H_2P-RB) were freshly prepared before measurement, by bubbling HCl(g) through the corresponding ZnP solution and adding triethylamine in excess to fully convert H_4P^{2+} to H_2P. The extent of reaction was followed by absorption spectroscopy.

Spectroscopic measurements

Materials: All solvents [CH_2Cl_2, *N*,*N*-dimethylformamide (DMF), toluene (Labscan), 2-methyl-THF (Acros), $CHCl_3$, *n*-butanol, 1,4-dioxane (Merck)] were used as purchased, except THF (Merck), which was distilled over sodium. Unless stated otherwise, measurements were made at 20 °C. Low-temperature measurements were made in 2-methyl-THF by using a temperature-controlled Oxford LN_2-cryostat.

Methods: Absorption spectra were recorded on a Cary 4 Bio spectrophotometer. Fully corrected steady-state fluorescence spectra were recorded on a SPEX Fluorolog τ2 spectrofluorimeter. The concentration of the chromophores was kept at approximately 5 μM to exclude the possibility of intermolecular interactions and to insure that inner filter effects were negligible. To facilitate immediate comparison of the fluorescence spectra, the optical densities of the samples were matched at the excitation wavelength (D = ZnP: $\lambda = 538$ – 548 nm, dependent upon solvent; D = H_2P: $\lambda = 574$ nm). The spectra of the ZnP compounds, and therefore the choice of excitation wavelength, is dependent upon the solvents ability to complex with zinc.[59] The fluorescence spectra of the reference compounds (ZnP-RB and H_2P-RB) were scaled to take into account the partitioning of the incident excitation light between the donor and the FeP acceptor in the D-B-A systems. Quenching efficiencies were calculated from the decrease in integrated intensity of the donor fluorescence.

Fluorescence lifetimes were measured by the phase/modulation technique by using a SPEX Fluorolog $\tau 2$ spectrofluorimeter, with a diluted silica sol scattering solution as reference. Since the acceptor (FeP) is nonfluorescent, both D-B reference compounds and D-B-A systems were expected to show a single-exponential fluorescence decay model. On a logarithmic scale in the range 2 – 300 MHz, 20 modulation frequencies were selected and, for room-temperature measurements, the fluorescence was collected through a 550 nm cut-off filter. In the low-temperature measurements, the donor fluorescence was collected through either a 580 nm (ZnP-samples) or 630 nm (H_2P-samples) band-pass filter. Lines from an argon ion laser (Spectra Physics 165 – 08) were used for excitation: 528.7 nm for the ZnP-samples and 514.5 nm for the H_2P-samples. For all room temperature measurements, the observed demodulations and phase shifts could be satisfactorily fitted to a single-exponential decay model. In frequency domain measurements it is not the absolute value of χ^2, but rather the change in χ^2 with different models that is used as an indication of goodness-of-fit.[70] Therefore, the goodness-of-fit was evaluated from the value of χ^2 and by visual inspection of the fit to the data points. In the low-temperature measurements, a small component with a much longer lifetime than expected was found (approximately equal for similar systems at the same temperature), and was attributed to instrumental artifacts.

Nanosecond transient absorption spectra and kinetic traces were recorded by using an Applied Photophysics flash-photolysis instrument. The pump pulse was the second harmonic of a Nd:YAG laser (Spectron Laser Systems, SL803G, 532 nm) with a pulse width of about 10 ns fwhm. The pump and probe beams were at right angles, and the excited triplet states were probed with a xenon arc lamp. The solvent used was 2-methyl-THF, and all samples were degassed by five freeze-pump-thaw cycles to a final pressure of 10^{-4} mbar. The concentrations used were the same as in absorption and fluorescence measurements. Kinetic traces were recorded at five different wavelengths from 440 to 480 nm (D = H_2P) and 450 to 490 nm (D = ZnP).

Transient absorption spectra on the picosecond timescale were recorded using the pump-probe technique. Excitation pulses at 545 nm and a 5 kHz repetition rate were provided by quadrupling the frequency of the idler output of an optical parametric amplifier (Spectra Physics, OPA-800) pumped by a Ti:Sapphire regenerative amplifier (Positive Light, Spitfire). The regenerative amplifier was pumped by a Nd:YLF laser (Positive Light, Merlin) and seeded by a mode-locked Ti:Sapphire laser (Spectra Physics, Tsunami), which in turn was pumped by a CW frequency-doubled diode-pumped Nd:YAG laser (Spectra Physics, Millennia V). The excitation beam, with a pulse energy of 240 nJ at the sample, was chopped at 170 Hz and sent through a computer-controlled optical delay line. A fraction of the output from the regenerative amplifier was focused into a 2 mm sapphire plate to generate a white light continuum, which was split into probe and reference beams. The continuum beams were focused onto the sample with spherical mirrors and then onto the slit of a computer-controlled monochromator (ISA, TRIAX 190) with an achromatic lens. Three silicon photodiodes (EKSPLA, FD-4) were used to monitor the intensity of the probe, reference, and pump beams. Transient absorption spectra were recorded between 490 and 740 nm with a 2 nm step size and monochromator bandwidth of 3.6 nm. The polarization of the pump beam was set at the magic angle by a Berek compensator (New Focus), and the probe beams passed through a cube polarizer after the sample. The sample was held in a static 1 mm path length cuvette and the concentration was approximately 160 μM.

Quantum mechanical calculations: The molecular orbitals of the D-B-A systems were calculated by using the PM3[71] semiempirical method as implemented in the program package HyperChem.[72] Lacking parameters for high-spin iron, the molecular orbitals were calculated for ZnP-RB-ZnP systems, which can be expected to be similar in structure to the ZnP-RB-FeP and H_2P-RB-FeP systems studied. For simplicity, alkyl chains in the porphyrin moieties as well as *tert*-butyl groups were omitted in the calculations. The geometry of the D-B-A systems was taken from the PM3 geometry-optimized components (ZnP and RB), and the phenyl groups and/or the central unit (R in Figure 1) were then rotated to obtain various conformations (Figure 6). Potential energy curves of these conformations were previously calculated on the fully optimized components.[28]

Acknowledgements

This work was supported by grants from the Swedish Natural Science Research Council (NFR), the Swedish Research Council for Engineering Sciences (TFR), and the Carl Trygger Foundation. K.K. is grateful to the Danish Research Agency (Århus) for a fellowship. We thank Dr. Gunnar Stenhagen for help with the mass spectrometry.

[1] M. R. Shortreed, S. F. Swallen, Z.-Y. Shi, W. Tan, Z. Xu, C. Devadoss, J. S. Moore, R. Kopelman, *J. Phys. Chem. B* **1997**, *101*, 6318 – 6322.
[2] J. Seth, V. Palaniappan, T. E. Johnson, S. Prathapan, J. S. Lindsey, D. F. Bòcian, *J. Am. Chem. Soc.* **1994**, *116*, 10578 – 10592.
[3] F. R. Li, S. I. Yang, Y. Z. Ciringh, J. Seth, C. H. Martin, D. L. Singh, D. H. Kim, R. R. Birge, D. F. Bocian, D. Holten, J. S. Lindsey, *J. Am. Chem. Soc.* **1998**, *120*, 10001 – 10017.
[4] T. Aida, D. L. Jiang, E. Yashima, Y. Okamoto, *Thin Solid Films* **1998**, *331*, 254 – 258.
[5] H. Kurreck, M. Huber, *Angew. Chem.* **1995**, *107*, 929 – 947; *Angew. Chem. Int. Ed. Engl.* **1995**, *34*, 849 – 866.
[6] D. Gust, T. A. Moore, A. L. Moore, *Pure Appl. Chem.* **1998**, *70*, 2189 – 2200.
[7] Y. Z. Hu, S. Tsukiji, S. Shinkai, S. Oishi, I. Hamachi, *J. Am. Chem. Soc.* **2000**, *122*, 241 – 253.
[8] L. Sun, M. K. Raymond, A. Magnuson, D. LeGourriérec, M. Tamm, M. Abrahamsson, P. H. Kenéz, J. Mårtensson, G. Stenhagen, L. Hammarström, S. Styring, B. Åkermark, *J. Inorg. Biochem.* **2000**, *78*, 15 – 22.
[9] V. Balzani, F. Scandola, *Supramolecular Chemistry*, Ellis Horwood, Chichester (UK) **1991**.
[10] A. S. Lukas, S. E. Miller, M. R. Wasielewski, *J. Phys. Chem. B* **2000**, *104*, 931 – 940.
[11] G. McDermott, S. M. Prince, A. A. Freer, A. M. Hawthornthwaite-Lawless, M. Z. Papiz, R. J. Cogdell, *Nature* **1995**, *374*, 517 – 521.
[12] V. Sundström, T. Pullerits, R. van Grondelle, *J. Phys. Chem. B* **1999**, *103*, 2327 – 2346.
[13] R. Huber, *Angew. Chem.* **1989**, *101*, 849 – 871; *Angew. Chem. Int. Ed. Engl.* **1989**, *28*, 848 – 869.
[14] S. Speiser, *Chem. Rev.* **1996**, *96*, 1953 – 1976.
[15] M. R. Wasielewski, *Chem. Rev.* **1992**, *92*, 435 – 461.
[16] A. Helms, D. Heiler, G. McLendon, *J. Am. Chem. Soc.* **1992**, *114*, 6227 – 6238.
[17] A. D. Joran, B. A. Leland, G. G. Geller, J. J. Hopfield, P. B. Dervan, *J. Am. Chem. Soc.* **1984**, *106*, 6090 – 6092.
[18] A. Osuka, N. Tanabe, S. Kawabata, I. Yamazaki, Y. Nishimura, *J. Org. Chem.* **1995**, *60*, 7177 – 7185.
[19] A. Osuka, F. Kobayashi, K. Maruyama, N. Mataga, T. Asahi, T. Okada, I. Yamazaki, Y. Nishimura, *Chem. Phys. Lett.* **1993**, *201*, 223 – 228.
[20] Y. Sakata, H. Tsue, M. P. O'Neil, G. P. Wiederrecht, M. R. Wasielewski, *J. Am. Chem. Soc.* **1994**, *116*, 6904 – 6909.
[21] H. Tamiaki, K. Nomura, K. Maruyama, *Bull. Chem. Soc. Japan* **1994**, *67*, 1863 – 1871.
[22] J. M. DeGraziano, A. N. Macpherson, P. A. Liddell, L. Noss, J. P. Sumida, G. R. Seely, J. E. Lewis, A. L. Moore, T. A. Moore, D. Gust, *New J. Chem.* **1996**, *20*, 839 – 851.
[23] G. L. I. Gaines, M. P. O'Neil, W. A. Svec, M. P. Niemczyk, M. R. Wasielewski, *J. Am. Chem. Soc.* **1991**, *113*, 719 – 721.
[24] A. Harriman, V. Heitz, M. Ebersole, H. van Willigen, *J. Phys. Chem.* **1994**, *98*, 4982 – 4989.
[25] A. Harriman, F. Odobel, J.-P. Sauvage, *J. Am. Chem. Soc.* **1995**, *117*, 9461 – 9472.
[26] P. Finckh, H. Heitele, M. Volk, M. E. Michel-Beyerle, *J. Phys. Chem.* **1988**, *92*, 6584 – 6590.
[27] L. R. Khundkar, J. W. Perry, J. E. Hanson, P. B. Dervan, *J. Am. Chem. Soc.* **1994**, *116*, 9700 – 9709.
[28] K. Kilså, J. Kajanus, J. Mårtensson, B. Albinsson, *J. Phys. Chem. B* **1999**, *103*, 7329 – 7339.
[29] S. I. Yang, J. Seth, T. Balasubramanian, D. Kim, J. S. Lindsey, D. Holten, D. F. Bocian, *J. Am. Chem. Soc.* **1999**, *121*, 4008 – 4018.
[30] M. Asano-Someda, Y. Kaizu, *Inorg. Chem.* **1999**, *38*, 2303 – 2311.

  0947-6539/01/0710-2132 $ 17.50+.50/0

[31] N. Toyama, M. Asano-Someda, T. Ichino, Y. Kaizu, *J. Phys. Chem. A* **2000**, *104*, 4857–4865.
[32] A. Osuka, K. Maruyama, N. Mataga, T. Asahi, I. Yamazaki, N. Tamai, *J. Am. Chem. Soc.* **1990**, *112*, 4958–4959.
[33] C. F. Portela, J. Brunckova, J. L. Richards, B. Schollhorn, Y. Iamamoto, D. Magde, T. G. Traylor, C. L. Perrin, *J. Phys. Chem. A* **1999**, *103*, 10540–10552.
[34] N. Mataga, H. Yao, T. Okada, Y. Kanda, A. Harriman, *Chem. Phys.* **1989**, *131*, 473–480.
[35] P. J. F. de Rege, S. A. Williams, M. J. Therien, *Science* **1995**, *269*, 1409–1413.
[36] L. X. Chen, P. L. Lee, D. Gosztola, W. A. Svec, P. A. Montano, M. R. Wasielewski, *J. Phys. Chem. B* **1999**, *103*, 3270–3274.
[37] D. Heiler, G. McLendon, P. Rogalskyj, *J. Am. Chem. Soc.* **1987**, *109*, 604–606.
[38] J. Kajanus, S. B. van Berlekom, B. Albinsson, J. Mårtensson, *Synthesis* **1999**, 1155–1162.
[39] R. W. Wagner, T. E. Johnson, F. Li, J. S. Lindsey, *J. Org. Chem.* **1995**, *60*, 5266–5273.
[40] R. Young, C. K. Chang, *J. Am. Chem. Soc.* **1985**, *107*, 898–909.
[41] H. M. Goff in *Iron Porphyrins*, *Part 1* (Eds.: A. B. P. Lever, H. B. Gray), Addison-Wesley, Reading, MA **1983**, Chapter 4.
[42] K. K. Jensen, S. B. van Berlekom, J. Kajanus, J. Mårtensson, B. Albinsson, *J. Phys. Chem. A* **1997**, *101*, 2218–2220.
[43] A. Harriman, G. Porter, A. Wilowska, *J. Chem. Soc. Faraday Trans. 2* **1983**, *79*, 807–816.
[44] J. Andréasson, H. Zetterqvist, J. Kajanus, J. Mårtensson, B. Albinsson, *J. Phys. Chem. A* **2000**, *104*, 9307–9314.
[45] J. Andréasson, J. Kajanus, J. Mårtensson, B. Albinsson, *J. Am. Chem. Soc.* **2000**, *122*, 9844–9845.
[46] T. Förster, *Naturwissenschaften* **1946**, *33*, 166–175.
[47] T. Förster, *Ann. Physik* **1948**, *2*, 55–75.
[48] R. Dale, J. Eisinger in *Biochemical Fluorescence: Concepts* (Eds.: R. F. Chen, H. Edelhoch), Marcel Dekker, New York **1975**, pp. 115–284.
[49] M. Gouterman in *The porphyrins, Vol. III* (Ed.: D. Dolphin), Academic Press, New York **1978**, Chapter 1.
[50] *Handbook of Chemistry and Physics*, CRC Press, Boca Raton, Florida, **1994**.
[51] R. A. Marcus, *J. Chem. Phys.* **1956**, *24*, 966–978.
[52] V. G. Levich in *Advances in Electrochemisty and Electrochemical Engineering, Vol. 4* (Ed.: P. Delahay), Interscience, New York **1966**, pp. 249–371.
[53] R. A. Marcus, N. Sutin, *Biochim. Biophys. Acta* **1985**, *811*, 265–322.
[54] R. A. Marcus, *Can. J. Chem.* **1959**, *37*, 155–163.
[55] R. A. Marcus, *J. Chem. Phys.* **1965**, *43*, 679–701.
[56] D. Rehm, A. Weller, *Ber. Bunsenges. Phys. Chem.* **1969**, *73*, 834–839.
[57] D. Rehm, A. Weller, *Isr. J. Chem.* **1970**, *8*, 259–271.
[58] A. Weller, *Z. Phys. Chem.* **1982**, *133*, 93–98.
[59] K. Kilså, A. N. Macpherson, T. Gillbro, J. Mårtensson, B. Albinsson, *Spectrochim. Acta A*, in press.
[60] R. H. Felton in *The Porphyrins, Vol. V* (Ed.: D. Dolphin), Academic Press, New York **1978**, Chapter 3.
[61] S. Larsson, *J. Chem. Soc. Faraday Trans. 2* **1983**, *79*, 1375–1388.
[62] N. Ivashin, B. Källebring, S. Larsson, Ö. Hansson, *J. Phys. Chem. B* **1998**, *102*, 5017–5022.
[63] A. M. Brun, A. Harriman, V. Heitz, J.-P. Sauvage, *J. Am. Chem. Soc.* **1991**, *113*, 8657–8663.
[64] H. Imahori, K. Hagiwara, M. Aoki, T. Akiyama, S. Taniguchi, T. Okada, M. Shirakawa, Y. Sakata, *J. Am. Chem. Soc.* **1996**, *118*, 11771–11782.
[65] K. Kilså, S. Larsson, B. Albinsson, unpublished results.
[66] R. L. Brookfield, H. Ellul, A. Harriman, *J. Chem. Soc. Faraday Trans. 2* **1985**, *81*, 1837–1848.
[67] K. S. Suslick, R. A. Watson, *New J. Chem.* **1992**, *16*, 633–642.
[68] K. Kumar, I. V. Kurnikov, D. N. Beratan, D. H. Waldeck, M. B. Zimmt, *J. Phys. Chem. A* **1998**, *102*, 5529–5541.
[69] K. Kilså, J. Kajanus, A. N. Macpherson, J. Mårtensson, B. Albinsson, *J. Am. Chem. Soc.*, in press.
[70] J. R. Lakowicz, *Principles of Fluorescence Spectroscopy*, Kluwer Academic/Plenum, New York, **1999**.
[71] J. J. P. Stewart, *J. Comp. Chem.* **1989**, *99*, 8127–8134.
[72] HyperChem, HyperCube, 1115 NW 4th Street, Gainesville, Florida 32601 (USA).

Received: October 4, 2000 [F2779]